Soft Matter

PAPER

View Article Online
View Journal | View Issue

Cite this: *Soft Matter*, 2022, **18**, 4963

Biomass-derived isosorbide-based thermoresponsive hydrogel for drug delivery†

Sebastian Bonardd, ‡[ab] Binoy Maiti,‡[c] Santiago Grijalvo, [d] Jacqueline Rodríguez, [ab] Hamidreza Enshaei,[e] Galder Kortaberria,[f] Carlos Alemán [eg] and David Díaz Díaz *[abh]

Received 13th May 2022,
Accepted 10th June 2022

DOI: 10.1039/d2sm00623e

rsc.li/soft-matter-journal

Herein, we describe the design and synthesis of a new variety of bio-based hydrogel films using a Cu(I)-catalyzed photo-click reaction. These films exhibited thermal-triggered swelling–deswelling and were constructed by crosslinking a triazide derivative of glycerol ethoxylate and dialkyne structures derived from isosorbide, a well-known plant-based platform molecule. The success of the click reaction was corroborated through infrared spectroscopy (FTIR) and the smooth surface of the obtained films was confirmed by scanning electron microscopy (SEM). The thermal characterization was carried out in terms of thermogravimetry (TGA) and differential scanning calorimetry (DSC), from which the decomposition onset and glass transition temperatures were determined, respectively. Additionally, mechanical properties of the samples were estimated by stress–strain experiments. Then, their swelling and deswelling properties were systematically examined in PBS buffer, revealing a thermoresponsive behavior that was successfully tested in the release of the anticancer drug doxorubicin. We also confirmed the non-cytotoxicity of these materials, which is a fundamental aspect for their potential use as drug carriers or tissue engineering matrices.

1. Introduction

Drug delivery technologies are rapidly developing fields and constitute an important component of nanomedicine drug development and therapeutics.[1,2] Controlled-release systems are designed to deliver drugs at predetermined rates for desirable times or specific sites, and the use of polymers is increasing nowadays in this area.[3] Such polymeric matrices are capable of modifying the biokinetic behavior of the transported bioactive molecule increasing its efficacy and stability, and reducing cytotoxicity on healthy peripheral tissues.

Within this context, hydrogels are a special class of polymeric networks, which can absorb and retain a large amount of water while preserving their three-dimensional integrity. Due to their high water content, many hydrogels are biocompatible and show similar properties to natural tissue, which makes them suitable for biomedical applications.[4–8] In recent years, increasing attention have been paid to stimuli-responsive hydrogels that can sense and respond to external stimuli, such as temperature, pH, light, electrical fields, *etc.*[9–12] In particular, thermoresponsive hydrogels are one class of the most widely studied stimuli-responsive hydrogels with great potential for drug delivery systems.[13–16]

Recently, we have reported the synthesis of a new series of hydrogels composed of glycerol ethoxylate and bisphenol A-based monomers.[17] The water-swollen hydrogel membranes displayed thermoresponsive actuation and lower critical solution temperature (LCST). In this work, motivated by the potential of these materials as drug delivery systems, and considering the potential toxicity of bisphenol A-derivatives, we decided to redesign the formulation using glycerol ethoxylate and biomass-derived isosorbide monomers.

[a] *Departmento de Química Orgánica, Universidad de La Laguna, Avda. Astrofisico Francisco Sánchez 3, La Laguna 38206, Tenerife, Spain. E-mail: ddiazdiaz@ull.edu.es*
[b] *Instituto Universitario de Bio-Orgánica Antonio González, Universidad de La Laguna, Avda. Astrofisico Francisco Sánchez 2, La Laguna 38206, Tenerife, Spain*
[c] *School of Chemistry & Biochemistry, Georgia Institute of Technology, 901 Atlantic Dr NW, Atlanta, GA, 30332, USA*
[d] *Networking Center on Bioengineering, Biomaterials and Nanomedicine (CIBER-BBN), Jordi Girona 18-26, 08034 Barcelona, Spain*
[e] *Departament d'Enginyeria Química and Barcelona Research Center in Multiscale Science and Engineering, IMEM-BRT, EEBE, Universitat Politècnica de Catalunya, C/Eduard Maristany, 10-14, Ed. I, 08019, Barcelona, Spain*
[f] *Materials + Technologies'' Group, Chemical & Environmental Engineering Department, Basque Country University, Plaza Europa 1, 20018, Donostia, Spain*
[g] *Institute for Bioengineering of Catalonia (IBEC), The Barcelona Institute of Science and Technology, Baldiri Reixac 10-12, 08028, Barcelona, Spain*
[h] *Institute of Organic Chemistry, University of Regensburg, Universitätstr. 31, Regensburg 93053, Germany*

† Electronic supplementary information (ESI) available. See DOI: https://doi.org/10.1039/d2sm00623e

‡ These authors contributed equally to this work.

2. Experimental part

2.1. Materials

All reagents and solvents employed in this work were purchased from commercial suppliers and used as received: Glycerol ethoxylate ($M_n \approx 1000$ g mol^{-1}), D-isosorbide (98%), sodium azide (≥99.5%), propargyl bromide (80 wt% solution in toluene), $CuSO_4{\cdot}5H_2O$ (98%), 2,2-dimethoxy-2-phenylacetophenone (DMPA, 99%) and triethylamine (Et_3N, >99%) were obtained from Sigma–Aldrich. Methanesulfonyl chloride (98%) and doxorubicin hydrochloride (DOX·HCl, >95%) were supplied by TCI. *N*,*N*,*N*′,*N*″,*N*″-pentamethyldiethylenetriamine (PMDETA, >98%) and ammonium chloride (≥99.5%) were purchased from Merck. Thiazolyl blue tetrazolium bromide was purchased from Merck Sigma Aldrich (St. Louis, MO, USA), Dulbecco's Modified Eagle Medium (DMEM), phosphate-buffered saline (PBS), fetal bovine serum (FBS), and trypsin–EDTA were purchased from ThermoFischer Technologies (Waltham, MA, USA).

2.2. Characterization techniques

2.2.1. ^{1}H and ^{13}C nuclear magnetic resonance spectroscopy. ^{1}H and ^{13}C–NMR measurements were recorded in a Bruker Avance 500 at room temperature. Chemical shifts are reported in parts per million (ppm) using as reference the residual $CDCl_3$ peak, centered at 7.26 ppm. The notation employed for the multiplicity of detected signals in NMR experiments was the following: s = singlet, d = doublet, t = triplet, q = quartet, m = multiplet.

2.2.2. Fourier transform infrared spectroscopy (FTIR). FTIR spectra of hydrogel's precursors and hydrogel films were obtained using a Thermo Nicolet Avatar 360 FTIR spectrometer and a Nicolet Nexus 670 FTIR spectrometer equipped with a single horizontal Golden Gate ATR cell with ZnSe cell/crystal, respectively. All spectra were recorded between 4000 and 600 cm^{-1} after 20 scans with a resolution of 2 cm^{-1}.

2.2.3. Scanning electron microscopy (SEM). SEM micrographs of gold-coated samples were obtained in a ZEISS EVO 15 scanning electron microscope (Zeiss, Germany), operating at an acceleration voltage of 10 kV for imaging. The surface metallization of samples was conducted using a QUORUM Q150R S PLUS sputtering instrument.

2.2.4. Thermogravimetric analysis (TGA). The thermal characterization of samples was carried out in a TGA/SDTA851 Mettler–Toledo thermobalance. TGA thermograms were measured under Air/O_2 (80 : 20) atmosphere between 25 °C and 600 °C at a heating rate of 10 °C min^{-1} using a dried piece of hydrogel film.

2.2.5. Differential scanning calorimetry (DSC). DSC measurements were carried out using a METTLER TOLEDO DSC 821e provided with an electric intracooler as a refrigeration unit. DSC analysis of a 24 h swollen film was conducted using a heating program consisting of 6 consecutive steps described as follows: (i) dynamic heating process from 25 to 120 °C at 2 °C min^{-1}, (ii) dynamic heating process from 120 to 200 °C at 20 °C min^{-1}, (iii) static heating process maintaining 200 °C during 3 min, (iv) cooling process from 200 to −80 °C at 10 °C min^{-1}, (v) static cooling process maintaining −80 °C for 3 min, ending with a (vi) dynamic heating process from −80 to 100 °C at 10 °C min^{-1}.

2.2.6. UV-Vis spectroscopy (UV-Vis). UV-Vis spectra were collected from an UV-2450 SHIMADZU between 350 nm and 650 nm with a resolution of 2 nm.

2.2.7. Tensile testing. Mechanical properties of obtained films were measured using a Zwick Z2.5/TN1S testing machine in stress–strain experiments conducted at a deformation rate of 3 mm min^{-1}. Calculated parameters were averaged considering a minimum of 5 samples for each system, which were cut from films in dimensions of 10 × 1.5 × 0.15 mm (length, width and thickness).

2.3. Synthesis of monomers

Reactions performed to obtain the molecular precursors of hydrogels were carried out using degassed solvents and flame-dried glassware connected to a Schlenk line. The purification of intermediates and final products was achieved by using conventional protocols such as evaporation under reduced pressure, precipitation, and column chromatography (using as stationary phase silica gel with particle size 63–200 μm acquired from Sigma–Aldrich). The irradiation process was conducted on a RPR-100 Photochemical Reactor (Rayonet) equipped with six long ultraviolet lamp life (365 nm).

2.3.1. Triazide derivative of glycerol ethoxylate (1a). The synthesis of this precursor was performed in two consecutive steps. First, glycerol ethoxylate (5.00 g, 5.00 mmol) (ESI†) was dissolved in 150 mL of dry dichloromethane (DCM) and cooled at 0 °C. Then, Et_3N (3.48 mL, 25.00 mmol) was added and, under constant stirring, methanesulfonyl chloride (2.57 g, 23.00 mmol) was added dropwise into the cooled reaction mixture. After 18 h, the suspension was filtered to obtain a clear and homogeneous yellow solution, which was then washed twice with 100 mL of distilled water and once with 100 mL of brine. The organic phase was dried overnight using Na_2SO_4 and concentrated under reduce pressure affording the desired compound which was used in the next step without further purification.

The above mesityl derivative (4.00 g, 3.00 mmol) was dissolved in 50 mL of dry *N*,*N*-dimethylformamide (DMF), after which sodium azide (0.98 g, 15.00 mmol) was added in one single portion allowing the reaction to proceed under constant stirring at 70 °C overnight. After this time, the mixture was noted to be a fine white suspension that was filtered affording a clear, homogeneous yellow-brown supernatant. DMF was removed under reduce pressure and the resultant crude oil triturated with 100 mL of ethyl acetate. The mixture was then sonicated for 15 min and filtered using 30 mL medium fritted glass funnel. The achieved brown filtrate was washed twice with 100 mL of distilled water and once with 100 mL of brine. The organic phase was dried overnight using Na_2SO_4 and concentrated to afford the triazide derivative in 70% yield. Spectroscopic data were in good agreement with those reported in the literature.[18] ^{1}H NMR ($CDCl_3$): δ 3.64–3.54 (m, –CH_2–CH_2–O–), 3.33 (t, –CH_2–N_3).

NOTE: Although we have not experience any safety problem handling triazide **1a**, it should be emphasized that small organic azides can be heat- and shock-sensitive. As a general recommendation, they should never be distilled to dryness or stored in the absence of solvent.

2.3.2. Bis(alkyne) isosorbide (1b). This isosorbide derivate was synthesized following a previously reported protocol by Beghdadi *et al.* In a round bottom flask, D-isosorbide (2.00 g, 13.68 mmol) was dissolved in 20 mL of dry DMF. Under constant stirring, NaH (1.64 g, 68.40 mmol) was added, followed by the addition of propargyl bromide (7.70 mL, 68.00 mmol). The reaction was allowed to proceed at room temperature overnight. Then, the solvent was removed under reduce pressure, the residue extracted with ethyl acetate (2× 100 mL) and the organic phase washed successively with distilled water and brine. The organic phase was dried with Na_2SO_4 and concentrated to get crude compound, which was purified by column chromatography using ethyl acetate:hexane (2 : 1, v/v) as eluent. The final product was obtained as a pale-yellow viscous oil in 53% yield. Spectroscopic data were in good agreement with those reported in the literature.[19] ^{1}H NMR ($CDCl_3$): δ 4.62 (t, J = 5 Hz, 1H), 4.51 (d, J = 5 Hz, 1H), 4.31–4.10 (m, 6H), 3.97–3.89 (m, 3H), 3.57 (t, J = 10 Hz, 1H), 2.44 (m, 2H). ^{13}C NMR ($CDCl_3$): δ 86.03, 83.24, 80.20, 79.29, 79.15, 78.65, 75.24, 75.09, 73.10, 69.96, 57.60, 56.78.

2.4. Hydrogel films

2.4.1. Preparation of hydrogel films. Bio-based hydrogel films were prepared as follows: In a 5 mL glass vial protected from light, triazide glycerol ethoxylate (0.30 g, 0.84 mmol of azide groups) and isosorbide dialkyne (0.09 g, 0.84 mmol of alkyne groups) were mixed and well-dissolved in 0.5 mL of dry DMF containing $CuSO_4{\cdot}5H_2O$ (4.2 mg, 0.017 mmol, 0.02 equiv. of alkyne), PMDETA (5.8 mg, 0.034 mmol, 2 equiv. of Cu^{+2}) and DMPA (8.6 mg, 0.034 mmol, 0.04 equiv. of alkyne). The above mixture was disposed on glass Petri dishes (4.0 cm diameter) and UV irradiated (365 nm) for 90 min. After the irradiation step, the sample was annealed at 100 °C overnight in order to remove DMF. Then, so-formed membranes were incubated and gently stirred in 0.02 M EDTA aqueous solution (8 h), distilled water (8 h) and acetone (8 h), consecutively. The membranes were finally dried at 80 °C for 24 h affording flexible and transparent yellowish films.

2.4.2. Swelling and deswelling kinetics of hydrogel films. The ability of these bio-based hydrogels to absorb water was quantified in terms of the equilibrium swelling ratio parameter (SR_e), which is defined in eqn (1):

$$SR_e(\%) = \frac{W_t - W_d}{W_d} \times 100 \quad (1)$$

where W_d and W_t are defined as the weight of the sample completely dried and the weight of the sample after a period t immersed in the aqueous solution, respectively. Thereby, the maximum amount of absorbed water by the sample can be measured. The above experiment was carried out as follows: A piece of dry membrane, previously lyophilized during 24 h, was weighted in order to determine W_d, after which was immersed in a thermoregulated flask containing PBS buffer solution at 22 °C. Then, the swollen sample was taken out and carefully dried with wet tissue paper, aiming to remove all the non-absorbed solution from the films' surface and weighted to record W_t values at different time intervals. The experiment was ended after reaching a stable SR_e value.

Once the maximum swollen state was established, the deswelling process of these samples was evaluated in terms of the water retention parameter (WR, eqn (2)). The initially swollen sample of weight W_o, equilibrated at 22 °C, was rapidly transferred to a PBS buffer solution at 37 °C or 50 °C aiming to evaluate this process at two different temperatures. Then, similar to the above protocol, after different time intervals the film was withdrawn from the hot solution, gently dried with tissue paper and weighted to record W_t values.

$$WR(\%) = \frac{W_t - W_d}{W_o - W_d} \times 100 \quad (2)$$

2.4.3. Cytotoxicity of hydrogel films. HeLa cells were grown in DMEM supplemented with 10% FBS and were regularly passaged in order to maintain exponential growth. Prior to put in contact the hydrogel with cells, the film material was sterilized under ultraviolet for 2 h, submerged in DMEM (15 mL) and incubated at 37 °C overnight. HeLa cells were transferred to a 96-well plate (3×10^3 cells) in 200 μL to favor the adhesion process. DMEM was discharged from the wells and replaced by DMEM that was previously in contact with the material (200 μL). Three concentrations were selected (6.07, 3.03 and 0.76 mg mL^{-1}) and cells were incubated for 24 h at 37 °C. The media was removed and freshly DMEM (200 μL) was added again incubating both non-treated and treated cells for 12 h at 37 °C. Finally, a MTT solution (5 mg mL^{-1}) (20 μL) was added. HeLa cells were incubated for 3 h. DMEM was removed and the resulting formazan crystals were dissolved in 200 μL of DMSO. Absorbance was measured at 570 nm using a BioTek Synergy H1 Multimode Reader (Agilent, Santa Clara, CA, USA) and normalized cellular viabilities were obtained by analyzing the ratio between non-treated and treated cells. Experiments were carried out in triplicate (SD = 3).

2.4.4. Adsorption and release of doxorubicin. A piece of dried hydrogel membrane (≈ 80 mg) was placed into a glass vial containing 10 mL of DOX·HCl aqueous PBS buffer solution (1×10^{-4} M). Using a UV-VIS spectrophotometer, the diminishing of the drug solution's absorbance was recorded at constant intervals of time by following the band centered at 480 nm. These absorbances were transformed into concentration values through a calibration curve, allowing the calculation of the absorption efficiency parameter (AE) through eqn (3):

$$AE(\%) = \frac{[Drug]_o - [Drug]_t}{[Drug]_o} \times 100 \quad (3)$$

Where $[Drug]_o$ and $[Drug]_t$ are the concentrations of drug in the dissolution at the beginning of the experiment and at time t, respectively.

For release experiments, the above preswollen drug-loaded membranes were rinsed with PBS buffer prior to be introduced into glass vials containing 10 mL of PBS buffer solutions preheated at 37 °C and 50 °C. Immediately after membrane immersion, the absorbance of the supernatant was measured at different time intervals by extracting 1 mL of the receptor phase, while the total volume of the experiment was maintained by adding 1 mL of fresh PBS solution. Cumulative drug release profiles were used to evaluate the evolution of the process.

Additionally, three kinetic models were selected to fit to the cumulative DOX released as a function of time: (i) Peppas–Sahlin equation (eqn (4)); (ii) Weibull model (eqn (5)); and (iii) Korsmeyer–Peppas (eqn (6)). M_t and M_∞ are the cumulative and maximum of drug released at time "t". In eqn (4), K_1 is a constant that corresponds to the release rate of the diffusion process whereas K_2 corresponds to the polymer relaxation.[20] In Weibull equation model, K is a constant and b corresponds to the diffusion mechanism. A Fickian mechanism is described when $b \leq 0.75$. Other processes involving complex release mechanisms are described when $0.75 < b < 1$.[21] Finally, K_H is a constant value and n is the diffusional exponent, in the case of eqn 6.[22] An Excel plugin namely DDSolver[23] was used to evaluate the DOX release data and be interpreted with various kinetic models in order to estimate the appropriate release mechanism of DOX from the composite material.

$$\frac{M_t}{M_\infty} = K_1 \times t^m + K_2 t^{2m} \quad (4)$$

$$\frac{M_t}{M_\infty} = \alpha \times \left(1 - \exp\left(-kt^b\right)\right) \quad (5)$$

$$\frac{M_t}{M_\infty} = K_{KP} \times t^n \quad (6)$$

3. Results and discussion

The first part of the present work consisted in the preparation of the clickable triazide (**1a**) and dialkyne (**1b**) membrane precursors, which were successfully obtained following the standard synthetic routes shown in Scheme 1A and B. Then, based on our previous experience,[17] the fabrication of films was achieved by inducing the reaction between both precursors, from a reaction mixture in which the molar ratio [azide groups]/[alkyne groups] = 1 condition was fulfilled. This reticulation

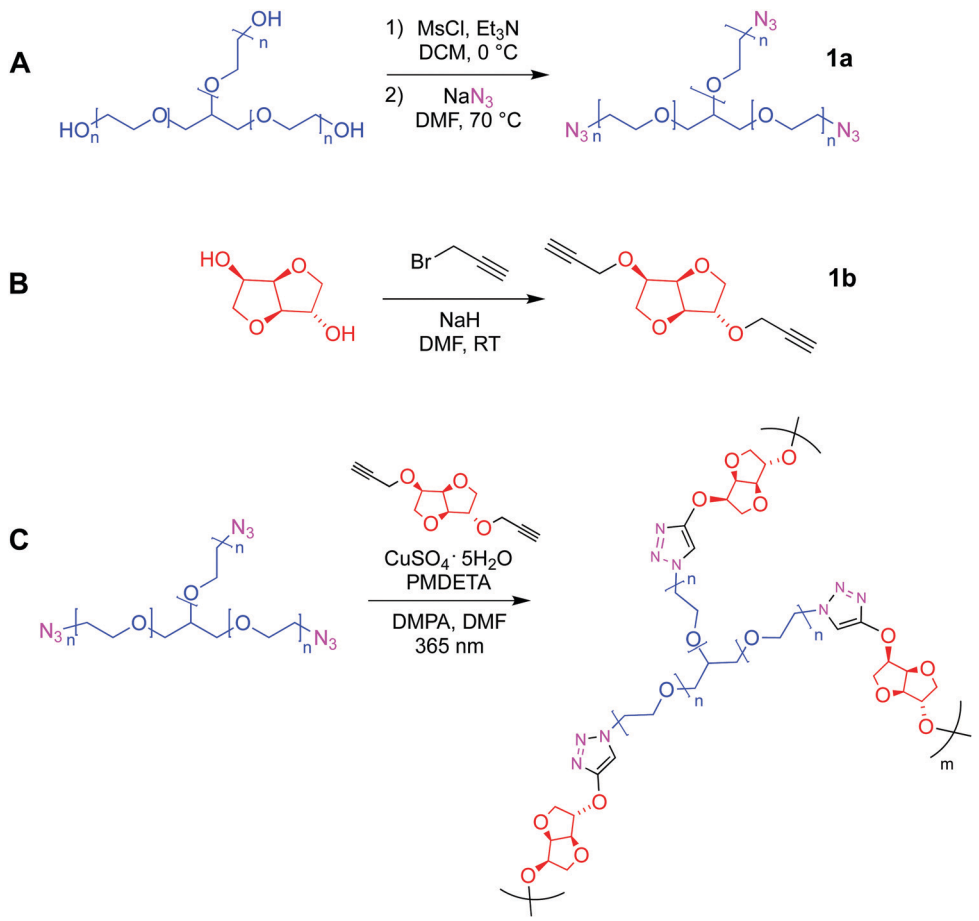

Scheme 1 Synthetic protocols employed in the preparation of (A) triazide glycerol ethoxylate and (B) bis-alkyne isosorbide derivates. (C) Synthesis of hydrogel films *via* Cu(I) mediated photo-click reaction.

process was achieved by means of a photo-triggered Cu(I)-catalyzed click reaction (Scheme 1C), where the generation of DMPA derived radicals mediated by light allows the photochemical reduction of Cu(II) to Cu(I) transient species that promote the cycloaddition process between terminal azide and alkyne moieties. It should be noted that in this case the use of photo-click chemistry enables an optimum homogenization of the reaction mixture during the polymerization.

Qualitatively, the success of this protocol was initially confirmed after obtaining a transparent and bendable solid film from both liquid precursors (Fig. 1A). A direct comparison between FTIR spectra recorded for **1a**, **1b** and the film can be conducted from Fig. 1B. The spectrum of the triazide precursor revealed an intense band centered at 2106 cm^{-1} demonstrating the presence of the azide group, while the presence of the terminal alkyne functionality in the isosorbide derivate was confirmed by the detection of a broad and high intensity band positioned around 3270 cm^{-1} (C–H vibration) as well as a low intensity signal centered at 2115 cm^{-1} (C≡C vibration mode). Moreover, as was expected, the FTIR spectra of both precursors allow the detection of aliphatic C–H vibrations appearing in the range between 3000–2800 cm^{-1} where, in the case of **1b**, two separated signals can be observed. This could be attributed to the cyclic structure of this precursor, which has been previously reported for other aliphatic cycles.[24] Furthermore, the presence of C–O–C linkages in both molecules was demonstrated through the presence of a strong and broad signal centered around 1120 and 1080 cm^{-1}. Using the above information, the FTIR analysis of films confirmed the success of the photo-click reaction due to the complete absence of signals ascribed to azides and alkynes functionalities, while bands related to the presence of C–H and C–O–C structures remained in the spectrum. In addition, a small group of signals (pointed by a black arrow in Fig. 1B) appeared between 1600–1500 cm^{-1} that could be assigned to the presence of triazole structures.[25–27] Finally, Fig. 1C exhibits a SEM image showing a smooth and homogeneous surface morphology, along with a rougher edge that could be caused by the cutting process used to prepare the sample.

After confirming the success of the light-triggered crosslinking process, the obtained films were subjected to stress–strain measurements in order to evaluate their mechanical properties (Fig. S1, ESI†). From the above results, values of 5.75 ± 1.55 MPa, 114.03 ± 27.22 MPa and 1.90 ± 0.12 MPa were calculated for stress at break, elongation at break and Young's modulus parameters, respectively. In previous works,[17] we have successfully carried out the reticulation of glycerol ethoxylate derivatives using diverse bifunctional molecules, such as bisphenol A diazide and 4,4′-methylenebis(cyclohexyl isocyanate), among others.[17] Thus, taking the aforementioned materials as reference, the values of the mechanical properties obtained in this work are within the same range as those obtained previously.[17] However, a deeper comparison between the obtained material and its previously published counterparts shows higher values of Young's modulus and stress at break, along with a lower elongation at break for the former. These parameters have been previously associated with the nature of the hard segments in these crosslinked materials,[17] which in this case would correspond to the isosorbide structure. Unlike the previously used molecules,[17] isosorbide is characterized by its lower size and its more strained structure. Thereby, the reticulation process of glycerol ethoxylate units by isosorbide-based structures seems to induce the formation of polymer films exhibiting greater mechanical strength but lower elongation capacity. Notwithstanding the above, with an elongation at break value above 100%, the as-prepared film can be considered as a material with an adequate elasticity. Furthermore, thermal properties of synthesized membrane was investigated by TGA and DSC (Fig. 2).

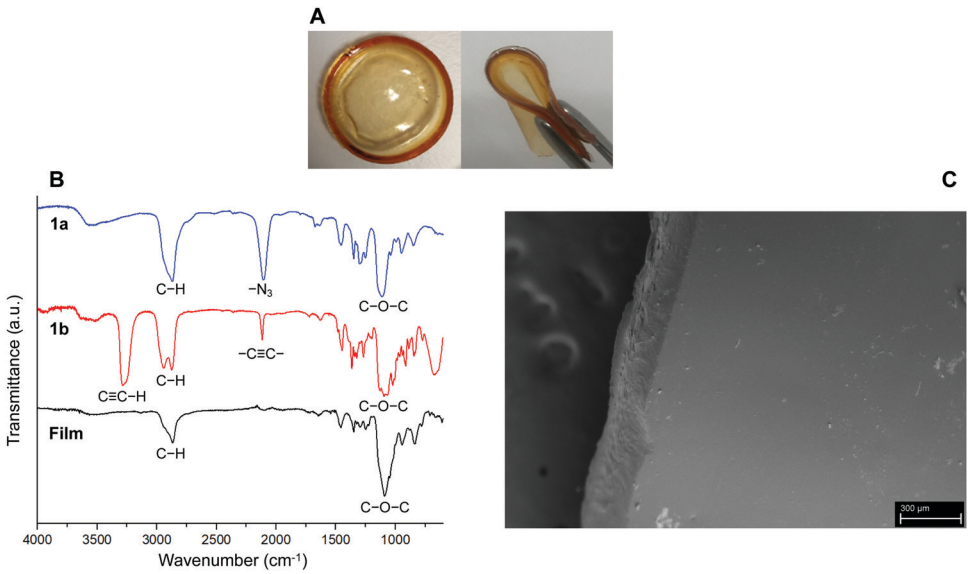

Fig. 1 (A) Digital images of obtained flexible hydrogel films (diameter of circular film = 4 cm). (B) FTIR spectra of **1a**, **1b** and the film. (C) SEM image of the hydrogel film. Scale bar = 300 µm.

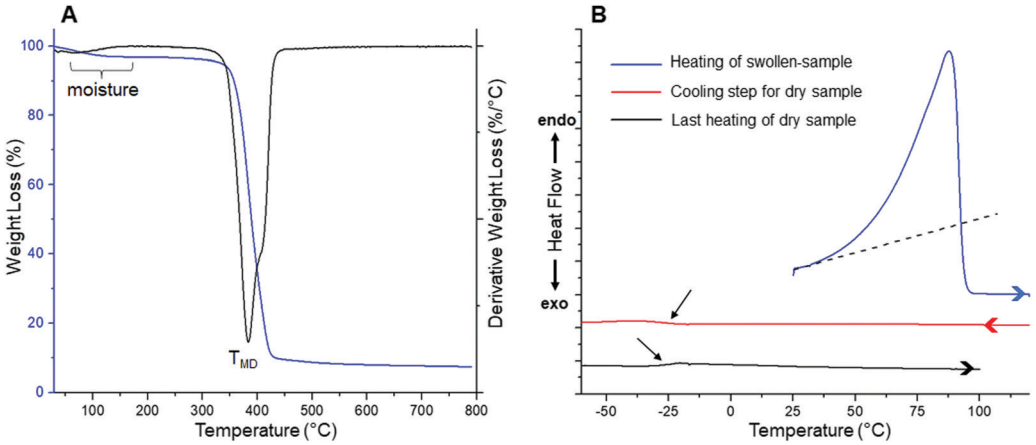

Fig. 2 (A) TGA and DTGA profiles obtained for a dry film. (B) DSC curves measured for a water-swollen sample.

TGA analysis reveals two weight loss steps, being the first one (centered at *ca.* 100 °C) assigned to the volatilization of adsorbed moisture and remaining water retained within the film coming from the washing process. In contrast, the second step would be ascribed to the degradation of the material itself. This decomposition is represented in the DTGA profile as a peak centered at 384 °C (labeled as T_{MD}), temperature at which the maximum degradation rate is reached. However, a more detailed analysis of the peak revealed that, at higher temperatures, its symmetry is broken accusing the presence of a third process merged with this degradation step. Considering the chemical structure of the material, abundant in ether bonds coming from both precursors, a feasible degradation mechanism could be interpreted as the random fragmentation of the polymer network through this type of linkages, giving way to the volatilization of low molecular weight species. In addition to the above, the merged process identified at higher temperatures could originate after the cleavage of more thermally stable chemical structures, such as remains of isosorbide-based entities and/or triazole units responsible for the crosslinking sites in the polymer matrix. Finally, the onset degradation temperature (T_{onset}), referred as the temperature at which the material loses 5% of its initial weight, occurs at 355 °C. Thus, this material meets most of the thermal requirements to be considered in a wide spectrum of applications, including biomedical ones. On the other hand, since DSC was carried out between temperatures where no degradation phenomena take place, we decided to conduct the experiment starting from a 24 h water-swollen film to study its thermal behavior in the presence and absence of water, aiming to start focusing the present study towards the analysis of these films in hydrogel state. It is well-known that PEG-based materials exhibit a LCST behavior which, in some cases, can be detected as an endothermic process during DSC measurements.[17,28–30] Above this temperature, hydrogen bonds between water molecules and polymer chains are disrupted, generating the dehydration of the material along with a phase separation that is usually evidenced by the appearance of turbidity in the sample. For pure PEG systems, the LCST behavior is achieved near to boiling conditions,[31,32] whereas by adjusting the amphiphilic nature of the system, for example, by adding hydrophobic structures into the polymer backbone, the LCST temperature can be notably decreased.[33,34] In previous works, by means of DSC, our group has been able to detect LCST temperatures in different glycerol ethoxylate membranes cross-linked with molecules of marked hydrophobic character.[17] Some of these membranes also acquired an opalescent appearance when heated above this temperature. Unfortunately, contrary to the above, in this case we were not capable of detect a clear LCST behavior instead, an intense and asymmetric endothermic peak centered at 87.6 °C was visualized during the heating process of the swollen film (Fig. 2B). This transition would be mostly related to the evaporation of water; however, it should be noted that the observed asymmetry is generated by a subtle increase of the recorded signal starting from temperatures far enough from volatilization processes ($\approx$ 35 °C, the dotted line in Fig. 2B is just for orientational purposes), therefore, we cannot discard the occurrence of other phenomena (*e.g.* water evaporation) that are eclipsed by the main signal at lower temperatures. We will complement this discussion later, during the evaluation of the swelling–deswelling properties of the material. Finally, after completing the first heating process, now the dry sample was subjected to two consecutive cooling and heating steps, in which a completely amorphous behavior was observed in the whole temperature range, detecting a glass transition temperature (T_g) centered at −27.1 °C (pointed by black arrows in Fig. 2B). After completing the structural, mechanical and thermal characterization of films, the properties of these materials as swellable hydrogels for drug delivery applications were evaluated (Fig. 3).

The first test conducted was the evaluation of the swelling kinetics during the immersion of a dried piece of material into PBS buffer at 22 °C. Fig. 3A exhibits the evolution of the swelling ratio (eqn (1)) through time showing that after 60 min of immersion a plateau is reached. This plateau is characterized by a maximum swelling ratio of 366%, being more than 3 times higher than the one previously reported for glycerol ethoxylate membranes reticulated with bisphenol entities.[17]

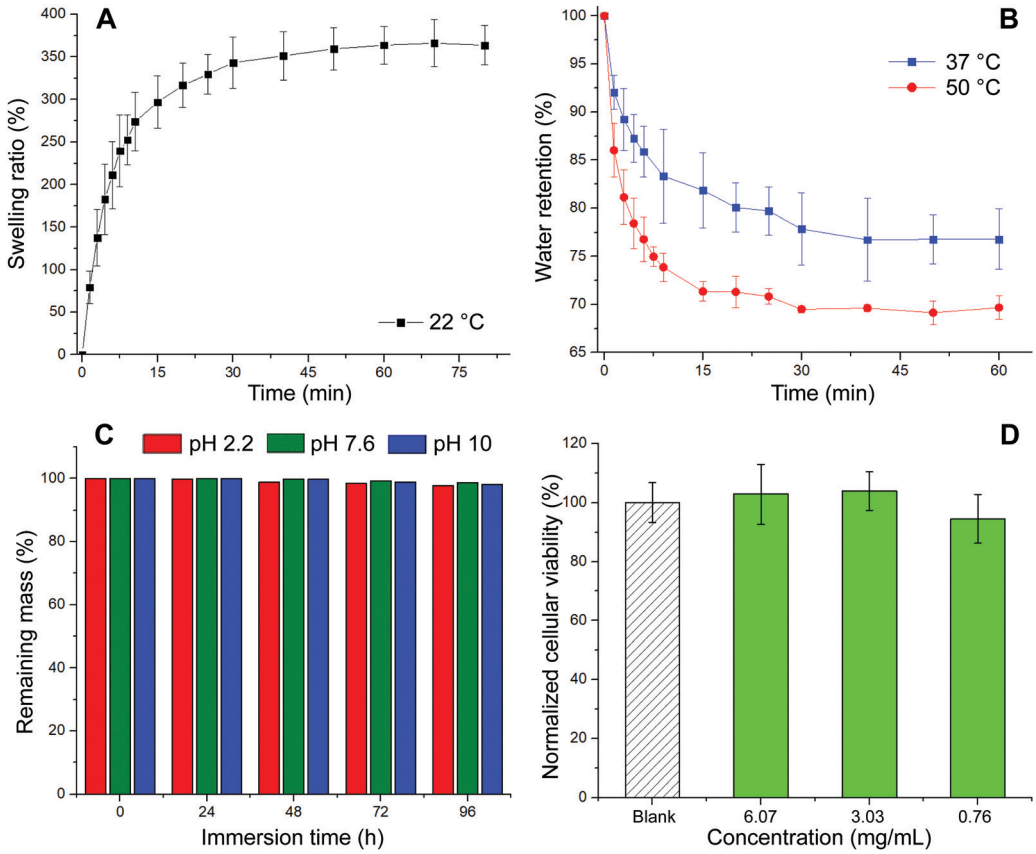

Fig. 3 (A) Evolution of swelling ratio and (B) water retention parameters as a function of time in PBS buffer solution. (C) Hydrogel stability over time measured at different pH values. (D) Cell-viability assay.

The hydrophobic character of the isosorbide-based monomer is lower than that of the bisphenol-based monomer. Therefore, by using isosorbide structures as crosslinking agents, the well-known hydrophilic property of glycerol ethoxylate would be less affected, being traduced not only in a higher swelling ratio but also in a faster swelling process. Then, the deswelling process of a fully PBS-swollen hydrogel film was evaluated at two temperatures, 37 °C and 50 °C, separately. Surprisingly, at both temperatures the hydrogel showed deswelling, being more pronounced at the higher temperature. The deswelling kinetics was achieved by measuring the evolution through time of the water retention parameter (eqn (2)), which results are shown in Fig. 3B. It can be seen that at both temperatures this parameter drops rapidly at the beginning of the process, and then gradually decreases as the hydrogel reaches a certain dehydrated state. More importantly, at higher temperatures, lower values are achieved, and the process takes place more rapidly. The calculated water retention values from the plateau regions were 77% and 69% at 37 °C and 50 °C, respectively. The value recorded at 50 °C is notably higher than the one previously reported for the system reticulated with bisphenol units, meaning that the deswelling process in this material is less pronounced. Again, this could be ascribed to the more hydrophilic character of the system which would require higher temperatures to favor the hydrogel dehydration. Although this system managed to exhibit a thermoresponsive behavior attributed to its swelling–deswelling ability, the markedly less favored deswelling process along with the absence of a clear LCST behavior could be related to the poor hydrophilic–hydrophobic balance achieved in the material. Nevertheless, we show that once the plateau value is reached, the water retention value can continue to decrease by transferring the sample to a warmer medium (Fig. S2, ESI†). Finally, the stability against the pH of these hydrogels was assessed by immersing them for prolongated times into different aqueous buffer solutions. Results displayed in Fig. 3C demonstrate that these materials, regardless the pH value, did not reveal quantifiable mass losses even after 96 h of incubation. Therefore, since no traces of material should be released to the surrounding media, we decided to attempt the evaluation of the biocompatible properties of our system in cell culture using the MTT assay[35] (Fig. 3D). Thus, high and low concentrations of the film (6.07, 3.03, and 0.76 mg mL^{-1}) were selected to study the effect induced by the material on cellular proliferation. To do so, HeLa cells were used as a model cell line and were incubated in the presence of appropriate material concentrations for 24 h at 37 °C. As shown in Fig. 3D, the three tested concentrations showed similar behavior if compared with non-treated cells with cellular viabilities over 90% suggesting that the material is non-cytotoxic. These results might confirm the potential use of our material for biomedical applications, supporting the idea

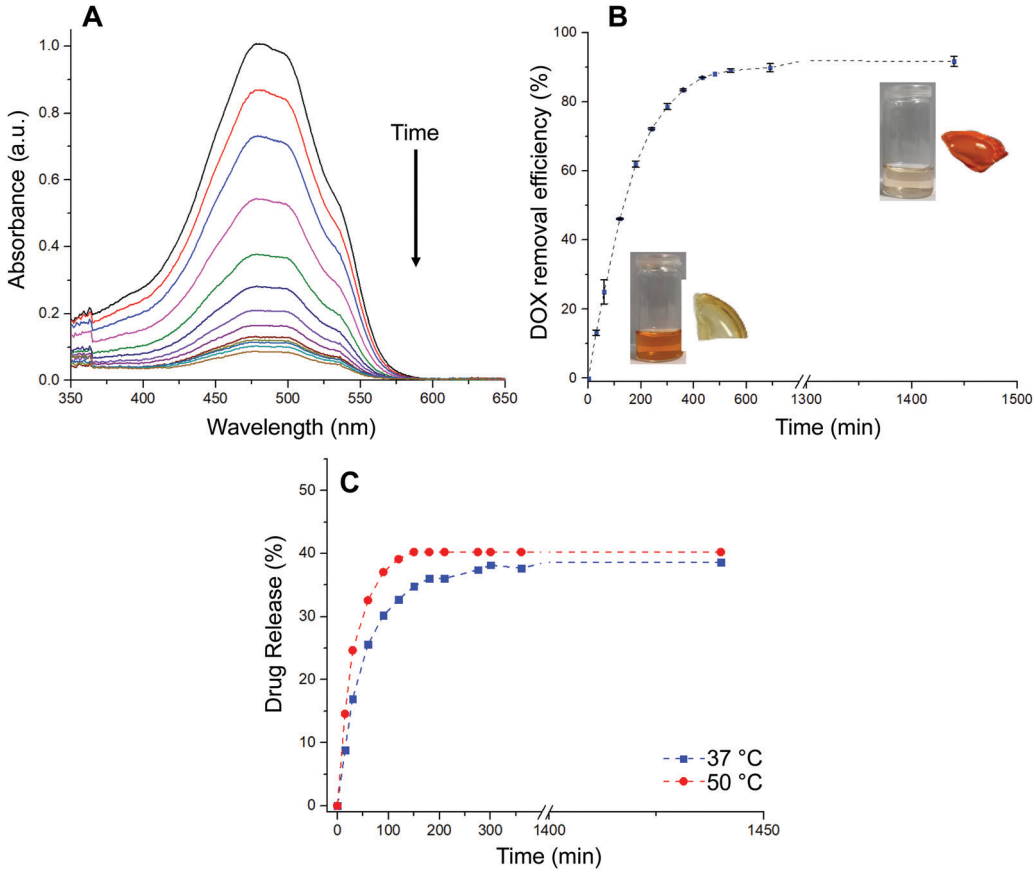

Fig. 4 (A) UV-Vis spectra recorded during drug adsorption. (B) Drug removal efficiencies measured as function of time. Insets: Photographs of the drug solution and pristine film (bottom-left) and the solution and drug-loaded film after the release experiment (top-right). (C) Drug release profiles conducted at different temperatures (37 °C and 50 °C).

of using isosorbide structures as crosslinking agents in PEG-based materials.

Finally, motivated by the thermoresponsive behavior showed by these hydrogels, along with their adequate biocompatibility, we test our material as a temperature-controlled delivery system using anticancer drug doxorubicin (Fig. 4).

The loading of the drug within hydrogel films was conducted by immersing a dry piece of sample into an aqueous PBS buffer solution of DOX·HCl. The process was followed by recording the absorbance of the supernatant at different time intervals as is shown in Fig. 4A. Moreover, aiming to a more quantitative analysis, the adsorption efficiency parameter (eqn (3)) was calculated and evaluated as function of time (Fig. 4B). The adsorption profile reveals that the material was able to remove from the solution 80% of the drug during the first 5 h of the experiment, approaching to a plateau state after 10 h. Based on the above, the dye adsorption efficiency after 24 h was 92%. During the process, the solution was gradually decolored while the hydrated film adopted an intense red color. It should be noted that, while the equilibrium swelling is reached at 60 min, the drug adsorption process continues for at least 10 more hours. Therefore, based on our results, it is plausible to infer that most of the drug adsorption takes place once the material reaches its maximum state of hydration. In this sense, the adsorption process would be mostly commanded by non-covalent interactions taking place between the drug and the hydrogel structure rather than water uptake. Then, the *in vitro* drug release of DOX-loaded hydrogels was evaluated in PBS buffer solution at 37 °C and 50 °C for 24 h (Fig. 4C). Interestingly, the encapsulated DOX displayed an initial burst release at early stage (17% and 25% in the first 30 min for incubations at 37 °C and 50 °C, respectively). The release profiles followed a controlled behavior in both cases reaching *a plateau* value within a period of 24 h. Specifically, the amount of DOX released was about 38% at 37 °C and 40% at 50 °C, respectively. As expected from deswelling measurements, release profiles obtained at 50 °C showed faster release kinetics along with slightly higher drug release. Thus, decreasing the temperature of the experiment from 50 to 37 °C enabled to increase the release time period from 150 to 300 min at which the maximum amount of drug is released.

Three models were used to describe the DOX release kinetics from the hydrogel film: (i) Peppas–Sahlin, (ii) Weibull distribution, and (iii) Korsmeyer–Peppas. These models have been extensively selected to give insight into the release mechanism of drugs from polymeric drug delivery systems making distinction between Fickian or non-Fickian diffusions. The release kinetic parameters are displayed in Table S1 (ESI†). The best

correlation coefficient (R^2) was obtained from the Weibull distribution (0.98) if compared with the Peppas–Sahlin (0.97) and Korsmeyer–Peppas (0.89) equations by plotting % cumulative DOX release against time (min). Taking the Weibull model as the most consistent one, we noticed the diffusion exponent was less than 0.75 (b = 0.56) indicating a Fickian diffusion mechanism of DOX (Fig. S3, ESI†). However, this model is empirical and faces some deficiencies[36] so the comparison with other semi-empirical release models is common. In this sense, we selected the Peppas–Sahlin model to describe the release behavior of DOX. This model showed a diffusional exponent m of 0.45 which confirmed the Fickian diffusion mechanism during the incubation process as described with Weibull.

4. Conclusions

In conclusion, bio-based hydrogel films can be rapidly fabricated by reacting a glycerol ethoxylate-based triazide and a dialkyne derived from isosorbide *via* Cu(I)-catalyzed photo-click reaction. These films are thermally stable up to *ca.* 350 °C and exhibit thermal-triggered swelling–deswelling behavior with a maximum swelling ratio of 366%, being also stable regardless the pH value. From a mechanical point of view, the films display values at break of 5.75 ± 1.55 MPa (stress), 114.03 ± 27.22 MPa (elongation) and a Young's modulus of 1.90 ± 0.12 MPa. The materials are non-cytotoxicity with cellular viabilities over 90% for a variety of concentrations. The foregoing properties make these materials suitable candidates for the delivery of therapeutic molecules. Thus, adsorption of anticancer drug doxorubicin can be achieved with an efficiency of 92% over 24 h. Subsequent release of doxorubicin is characterized by an initial burst release (*i.e.* 17% and 25% in the first 30 min for incubations at 37 °C and 50 °C, respectively), followed by a controlled release reaching *a plateau* value of *ca.* 40% within a period of 24 h. The fitting of the release kinetics to Korsmeyer–Peppas model suggest a quasi-Fickian diffusion mechanism of doxorubicin. We plan to carry out future studies for fine-tuning the thermoresponsive and release kinetics profile of this type of hydrogel films.

Conflicts of interest

There are no conflicts to declare.

Acknowledgements

Financial support from Universität Regensburg and Spanish Government (PID2019–105391GB–C21) is acknowledged. S.B. thanks MINECO for a Juan de la Cierva – Formación contract (FJC2019-039515-I). Authors thank Dr Beatriz Gil Hernández for assistance with IR equipment. D. D. D. thanks the Spanish Ministry of Science, Innovation and Universities for the Senior Beatriz Galindo Award (BEAGAL18/00166) and NANOtec, INTech, Cabildo de Tenerife and ULL for laboratory facilities. H.E. and C.A. are thanked to I + D + i project RTI2018-098951-B-I00 funded by MCIN/AEI/10.13039/501100011033/FEDER and the Agència de Gestió d'Ajuts Universitaris i de Recerca (2017SGR359) for financial support.

References

1 R. Langer and D. Tirrell, Designing materials for biology and medicine, *Nature*, 2004, **428**(6982), 487–492, DOI: **10.1038/nature02388**.
2 H. Rosen and T. Abribat, The rise and rise of drug delivery, *Nat. Rev. Drug Discovery*, 2005, **4**(5), 381–385, DOI: **10.1038/nrd1721**.
3 A. Hoffman, Hydrogels for biomedical applications, *Adv. Drug Delivery Rev.*, 2002, **54**(1), 3–12, DOI: **10.1016/s0169-409x(01)00239-3**.
4 K. Xue, X. Wang, P. W. Yong, D. J. Young, Y.-L. Wu, Z. Li and X. J. Loh, Hydrogels as emerging materials for translational biomedicine, *Adv. Ther.*, 2019, **2**(1), 1800088, DOI: **10.1002/adtp.201800088**.
5 S. Correa, A. K. Grosskopf, H. L. Hernández, D. Chan, A. C. Yu, L. M. Stapleton and E. A. Appel, Translational applications of hydrogels, *Chem. Rev.*, 2021, **121**(18), 11385–11457, DOI: **10.1021/acs.chemrev.0c01177**.
6 Y. S. Zhang and A. Khademhosseini, Advances in engineering hydrogels, *Science*, 2017, **356**(6337), eaaf3627, DOI: **10.1126/science.aaf3627**.
7 T. Hoare and D. Kohane, Hydrogels in drug delivery: Progress and challenges, *Polymer*, 2008, **49**(8), 1993–2007, DOI: **10.1016/j.polymer.2008.01.027**.
8 N. Peppas, J. Hilt, A. Khademhosseini and R. Langer, Hydrogels in biology and medicine: from molecular principles to bionanotechnology, *Adv. Mater.*, 2006, **18**(11), 1345–1360, DOI: **10.1002/adma.200501612**.
9 N. Peppas, P. Bures, W. Leobandung and H. Ichikawa, Hydrogels in pharmaceutical formulations, *Eur. J. Pharm. Biopharm.*, 2000, **50**, 27–46, DOI: **10.1016/s0939-6411(00)00090-4**.
10 Y. Qiu and K. Park, Environment-sensitive hydrogels for drug delivery, *Adv. Drug Delivery Rev.*, 2001, **53**, 321–339, DOI: **10.1016/s0169-409x(01)00203-4**.
11 P. Li, J. Zhang and C.-M. Dong, Photosensitive poly(o-nitrobenzyloxycarbonyl-l-lysine)-*b*-PEO polypeptide copolymers: synthesis, multiple self-assembly behaviors, and the photo/pH-thermo-sensitive hydrogels, *Polym. Chem.*, 2017, **8**, 7033–7043, DOI: **10.1039/c7py01574g**.
12 D.-L. Liu, X. Chang and C.-M. Dong, Reduction- and thermo-sensitive star polypeptide micelles and hydrogels for on-demand drug delivery, *Chem. Commun.*, 2013, **49**, 1229–1231, DOI: **10.1039/c2cc38343h**.
13 D. Schmaljohann, Thermo-and pH-responsive polymers in drug delivery, *Adv. Drug Delivery Rev.*, 2006, **58**(15), 1655–1670, DOI: **10.1016/j.addr.2006.09.020**.
14 C. Gong, T. Qi, X. Wei, Y. Qu, Q. Wu, F. Luo and Z. Qian, Thermosensitive polymeric hydrogels as drug delivery systems, *Curr. Med. Chem.*, 2013, **20**(1), 79–94, DOI: **10.2174/0929867311302010009**.

15 Y. Yu, Y. Cheng, J. Tong, L. Zhang, Y. Wei and M. Tian, Recent advances in thermo-sensitive hydrogels for drug delivery, *J. Mater. Chem. B*, 2021, **9**, 2979–2992, DOI: **10.1039/D0TB02877K**.

16 H. Huang, X. Qi, Y. Chen and Z. Wu, Thermo-sensitive hydrogels for delivering biotherapeutic molecules: A review, *Saudi Pharm. J.*, 2019, **27**(7), 990–999, DOI: **10.1016/j.jsps.2019.08.001**.

17 B. Maiti, A. Abramov, L. Franco, J. Puiggalí, H. Enshaei, C. Alemán and D. D. Díaz, Hydrogel actuators: Thermoresponsive shape-memory hydrogel actuators made by photo-triggered click chemistry, *Adv. Funct. Mater.*, 2020, **30**(24), 2070150, DOI: **10.1002/adfm.202070150**.

18 R. A. Wess and M. Becker, *Strain-promoted crosslinking of peg-based hydrogels via copper-free cycloaddition*, WO20140 22501A3, 2014.

19 C. Besset, J.-P. Pascault, E. Fleury, E. Drockenmuller and J. Bernard, Structure−properties relationship of biosourced stereocontrolled polytriazoles from click chemistry step growth polymerization of diazide and dialkyne dianhydrohexitols, *Biomacromolecules*, 2010, **11**(10), 2797–2803, DOI: **10.1021/bm100872h**.

20 N. A. Peppas and J. J. Sahlin, A simple equation for the description of solute release. III. Coupling of diffusion and relaxation, *Int. J. Pharm.*, 1989, **57**, 169–172, DOI: **10.1016/0378-5173(89)90306-2**.

21 V. Papadopoulou, K. Kosmidis, M. Vlachou and P. Macheras, On the use of the Weibull function for the discernment of drug release mechanisms, *Int. J. Pharm.*, 2006, **309**, 44–50, DOI: **10.1016/j.ijpharm.2005.10.044**.

22 P. L. Ritger and N. A. Peppas, A simple equation for description of solute release II. Fickian and anomalous release from swellable devices, *J. Controlled Release*, 1987, **5**(1), 37–42, DOI: **10.1016/0168-3659(87)90035-6**.

23 Y. Zhang, M. Huo, J. Zhou, A. Zou, W. Li, C. Yao and S. Xie, DDSolver: an add-in program for modeling and comparison of rug dissolution profiles, *AAPS J.*, 2010, **12**, 263–271, DOI: **10.1208/s12248-010-9185-1**.

24 R. C. Fort and P. v R. Schleyer, Adamantane: Consequences of the diamondoid structure, *Chem. Rev.*, 1964, **64**(3), 277–300, DOI: **10.1021/cr60229a004**.

25 S. G. Aziz, S. A. Elroby, A. Alyoubi, O. I. Osman and R. Hilal, Experimental and theoretical assignment of the vibrational spectra of triazoles and benzotriazoles. Identification of IR marker bands and electric response properties, *J. Mol. Model.*, 2014, **20**, 2078, DOI: **10.1007/s00894-014-2078-y**.

26 F. Dong, J. Zhang, C. Yu, Q. Li, J. Ren, G. Wang, G. Gu and Z. Guo, Synthesis of amphiphilic aminated inulin via 'click chemistry' and evaluation for its antibacterial activity, *Bioorg. Med. Chem. Lett.*, 2014, **24**(18), 4590–4593, DOI: **10.1016/j.bmcl.2014.07.029**.

27 T. Wenqiang, Q. Li, W. Li, F. Dong and Z. Guo, Synthesis and antioxidant property of novel 1,2,3-triazole-linked starch derivatives via 'click chemistry', *Int. J. Biol. Macromol.*, 2016, **82**, 404–410, DOI: **10.1016/j.ijbiomac.2015.10.007**.

28 B. Maiti, S. Maiti and P. De, Self-assembly of well-defined fatty acid based amphiphilic thermoresponsive random copolymers, *RSC Adv.*, 2016, **6**, 19322–19330, DOI: **10.1039/C6RA00336B**.

29 D. Roy, W. L. A. Brooks and B. S. Sumerlin, New directions in thermoresponsive polymers, *Chem. Soc. Rev.*, 2013, **42**, 7214–7243, DOI: **10.1039/C3CS35499G**.

30 C. Pelosi, E. Guazzelli, M. Calosi, L. Bernazzani, M. R. Tiné, C. Duce and E. Martinelli, Investigation of the LCST-thermoresponsive behavior of novel oligo(ethylene glycol)-modified pentafluorostyrene homopolymers, *Appl. Sci.*, 2021, **11**, 2711, DOI: **10.3390/app11062711**.

31 D. R. Yen, S. Raghavan and E. W. Merrill, Fractional precipitation of star poly(ethylene oxide), *Macromolecules*, 1996, **29**(27), 8977–8978, DOI: **10.1021/ma961184y**.

32 M. Nichols, *Factors affecting size and swelling of poly(ethylene glycol) hydrogel microspheres formed in aqueous sodium sulfate solutions* (2009), All Theses and Dissertations (ETDs), p. 485, **https://openscholarship.wustl.edu/etd/485**.

33 L. I. Ronco, A. Basterretxea, D. Mantione, R. H. Aguirresarobe, R. J. Minari, L. M. Gugliotta, D. Mecerreyes and H. Sardon, Temperature responsive PEG-based polyurethanes ''à la carte'', *Polymer*, 2017, **122**, 117–124, DOI: **10.1016/j.polymer.2017.06.043**.

34 H. Sardon, J. P. K. Tan, J. M. W. Chan, D. Mantione, D. Mecerreyes, J. L. Hedrick and Y. Y. Yang, Thermoresponsive random poly(ether urethanes) with tailorable LCSTs for anticancer drug delivery, *Macromol. Rapid Commun.*, 2015, **36**(19), 1761–1767, DOI: **10.1002/marc.201500247**.

35 T. Mosmann, Rapid colorimetric assay for cellular growth and survival: Application to proliferation and cytotoxicity assays, *J. Immunol. Methods*, 1983, **65**(1–2), 55–63, DOI: **10.1016/0022-1759(83)90303-4**.

36 M. J. Fabra, R. Pérez-Masiá, P. Talens and A. Chiralt, Influence of the homogenization conditions and lipid self-association on properties of sodium caseinate based films containing oleic and stearic acids, *Food Hydrocolloids*, 2011, **25**, 1112–1121, DOI: **10.1016/j.foodhyd.2010.10.008**.

